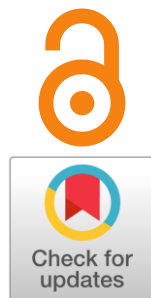


Solid state electrochemical devices for hydrogen energy

Anatoly Demin ^{a,b}, Dmitry Bronin ^{a,*}

Received: 14 June 2023
Accepted: 24 August 2023
Published online: 12 September 2023

DOI: [10.15826/elmattech.2023.2.016](https://doi.org/10.15826/elmattech.2023.2.016)



The idea of nuclear-hydrogen energy draws growing interest of power engineering specialists. One of the ways to implement such a direction of development is integration of nuclear power station and high temperature electrochemical devices, namely solid oxide electrolyzers (SOE) and fuel cells (SOFC). This paper reviews the principal features of the devices and their high efficiency of energy transformation. The electrical efficiency of the SOEs can exceed 100 % at the expense of high-grade potential heat energy consumed by the electrolyzer. The efficiency of the SOFCs amounts to 70 %. The state of the art of long-term tests of single cells of SOEs and SOFC stacks are presented.

Keywords: solid oxide electrolyte, solid oxide fuel cell, solid oxide electrolyzer, protonic ceramic fuel cell, protonic ceramic electrolytic cell, nuclear power station, nuclear hydrogen energy

© 2023, the Authors. This article is published in open access under the terms and conditions of the Creative Commons Attribution (CC BY) license <http://creativecommons.org/licenses/by/4.0/>.

1. Introduction

This publication aims to inform readers on the main characteristics of solid oxide electrolyzers (SOE) and solid oxide fuel cells (SOFC) which open up possibilities to increase the operation efficiency of nuclear stations. The performance characteristic of the solid state electrochemical devices is a prerequisite for the energy-economic models to combine the high temperature electrochemical devices and the nuclear power infrastructure. Brief information on electrochemical devices based on protonic ceramic electrolytes is also presented.

1.1. The nuclear-hydrogen energy

The wish of the humanity for the hydrogen energy in return of the energy obtained from the fossil fuel (coal,

oil, gas *at alias*) is hampered by the high cost of the hydrogen and the absence of the well-developed infrastructure corresponding to the new energy strategy. One of the benefits of the hydrogen energy is the minimum environmental impact preventing global warming, ambient air quality deterioration and the like.

At present, electrolysis of water is one of the most developed technologies that can provide large-scale non-polluting hydrogen production in the near future. The source of energy for electrolytic hydrogen production can be nuclear stations. On the October 25, 2018, academician N. N. Ponomarev-Stepnoy in his lecture on the "Prospect of the nuclear-hydrogen energy" observed that all of "Rosenergoatom JSC" nuclear stations (Balakovskaya, Beloyarskaya, Kalininskaya, Kolskaya, Kurskaya, Leningradskaya, Novovoronezhskaya, Rostovskaya, Smolenskaya) produce hydrogen for their own needs. The total hydrogen production capacity of those nuclear stations is around 530 m³/h. Therefore, the nuclear energetic energy is substantially ready for the

a: The Institute of High Temperature Electrochemistry, Yekaterinburg 620066, Russia

b: Ural Federal University, Yekaterinburg 620002, Russia

* Corresponding author: bronin@ihte.uran.ru

large-scale environmentally safe hydrogen production. The concept of hydrogen production by means of nuclear energy has been called “nuclear-hydrogen energy” [1, 2].

There is every reason to believe that high temperature water electrolysis at temperature higher than 500 °C up to 800–1000 °C is economically most efficient for hydrogen production. At such temperatures, both ohmic and polarization losses, and consequently the internal resistance of the electrolyzers, reduce considerably. At the expense of lower energy loss, the expenditure of electricity is much less than at low temperature electrolysis [3]. The use of nuclear energy can cut the hydrogen production costs even more.

For the first time, main issues of high temperature water electrolysis have been expanded in the collective monograph [4]. The review [5] may be proposed as a later publication. Some information on high temperature electrolyzers powered by nuclear stations is given in [3, 6–15].

1.2. Reversible fuel cells

Operation of a nuclear station in the base-load regime considerably enhances the power system safety. Cogeneration of electricity, hydrogen, and heat at nuclear stations can promote solution of an important problem: smoothing the electrical load curve, particularly nighttime valley, by means of hydrogen production and accumulation at night and hydrogen utilization during the peak load. It should be noted that high temperature solid oxide devices are capable of “reversible” operation, namely decompose water for hydrogen production (electrolyzer mode) at night or generate electricity from hydrogen (fuel cell mode) at the peak load. The availability of “reversible” fuel cells in the infrastructure of the power plants has been observed by many scientists [16–22]. There are convincing facts indicating lower degradation rate of the fuel cells tested in the reversible mode than in the only fuel cell or electrolyzer mode [23–26].

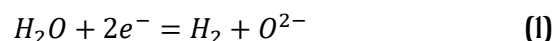
2. Solid oxide electrolyzers (SOEs)

The current state of developments in the field of hydrogen production by electrolysis, including high temperature solid oxide electrolysis, is reflected in [27].

The basis of SOE is a solid oxide electrolyte with oxygen ion conductivity at working temperatures (as a rule 700–900 °C). The most common electrolyte is yttria stabilized zirconia (YSZ). Nickel-cermet is traditionally used as a hydrogen electrode (cathode). The materials of the oxygen electrode (anode), as a rule, are compositions based on manganites, cobaltites, nickelites or ferrites

doped with REM oxides. The electrolyte must be gas-tight, and the electrodes must be porous. A constant voltage is applied to the electrodes, with positive potential at the anode.

Water vapor is supplied to the cathode space of the SOE. The cathode reaction at the SOE is as follows:



Hydrogen is the main product of water vapor electrolysis in the SOE. The concentration of water vapor in the cathode gas flow decreases as the flow moves, while the concentration of hydrogen increases. Complete decomposition of water vapor electrochemically is impossible. Wet hydrogen exits the cathode channel of the SOE. The completeness of decomposition is determined by the steam utilization factor (η_{H_2O}). Usually, $\eta_{H_2O} = 0.8 \div 0.9$. At the first stage moisture from the outgoing cathode stream is separated by condensation, to obtain dry hydrogen, the residual moisture is removed using silica gel.

As a result of reaction (2), pure oxygen is released at the SOE anode



which is a valuable by-product.

The theoretical foundations of high-temperature electrolysis are considered in [4]. The operating characteristics of the SOE are cell voltage (U), current (I), and temperature. The current density (i) in the cross-section x of the SOE, $i(x)$, is determined by the expression

$$i(x) = \frac{(U - E(x))}{\rho^*}, \quad (3)$$

where U is applied voltage, E is electromotive force (EMF), $\rho^* = \rho_{Ohm} + \rho_\eta$ is effective specific (referred to 1 cm²) cell resistance, ρ_{Ohm} is specific Ohmic resistance of an electrolyte and electrodes, ρ_η is specific polarization resistance of electrodes. In the case of steam electrolysis the EMF can be calculated by the formula

$$E_H = \left(\frac{RT}{2F} \right) \ln \left(\frac{K_1 p_{H_2}}{p_{H_2O}} \right), \quad (4)$$

where $R = 8,314 \text{ J}/(\text{mol} \cdot \text{K})$ is the gas constant, T is temperature in Kelvin, $F = 96,485 \text{ C/mol}$ is the Faraday constant, K_1 is the equilibrium constant of hydrogen oxidation reaction, p is partial pressure of corresponding components.

Since the concentration of hydrogen in the gas mixture increases as it moves in the cathode channel, the EMF increases and, consequently, the current density decreases along the cell. Therefore, in practice, the value of the cell average current density is used. Formula (3) can be used to calculate the average current density if the EMF value is replaced by its average value (E_{av}) within the cell. E_{av} decreases linearly with increasing temperature from

700 to 900 °C from 994 to 935 mV at $\eta_{H_2O} = 0.9$ and from 984 to 922 mV at $\eta_{H_2O} = 0.8$.

Since the effective resistance of the cell decreases with increasing temperature and the EMF decreases, the possibility of achieving high current densities increases and, as a result, the dimensions and material consumption of the SOE of a given productivity decrease. However, it should be taken into account that at a higher temperature the degradation rate of the properties of the SOE components (first of all, electrodes) increases, which leads to a deterioration in the characteristics of the SOE, and, in addition, the range of materials that can be used in the device narrows. Therefore, in practice, a compromise has to be found.

The general definition of efficiency is the ratio of produced energy to consumed energy. In the general case, the electric power (W) is converted into the chemical energy of the electrolysis products determined by the enthalpy of the oxidation reaction of the product ($-\Delta H$) and heat (Q) in the electrolyzer:

$$W = -\Delta H + Q. \quad (5)$$

The energy for obtaining one mole of hydrogen is calculated by the formula

$$W = 2FU, \quad (6)$$

where U is the cell voltage. A feature of SOE is the possibility of carrying out the process in the mode without heat release ($Q = 0$) and even in the mode of heat absorption ($Q < 0$). The first mode is called "thermoneutral" with the corresponding voltage (U_m), and the second mode – endothermic with $U < U_m$. When operating in the endothermic mode, part of the electrical energy is replaced by cheaper thermal energy. From (5) and (6) it follows that

$$U_{th} = \frac{-\Delta H_T}{2F}. \quad (7)$$

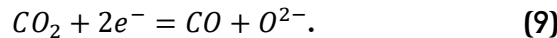
As follows from (6) and (7), the electrical efficiency of the SOE is equal to the ratio of the thermoneutral voltage to the voltage of the cell:

$$\eta = \frac{U_{th}}{U}. \quad (8)$$

At the working temperatures of the SOE (700–900 °C) $U_m \approx 1.29$ V. Specific electricity consumption is calculated by the formulas $W = k_m U$ and $W = k_V U$, where $k_m = 26.592 \text{ kWh}/(\text{kgH}_2 \cdot \text{V})$ and $k_V = 2.392 \text{ kWh}/(\text{Nm}^3 \text{H}_2 \cdot \text{V})$. Under thermoneutral regime, $W = 34.2 \text{ kWh}/(\text{kgH}_2)$ and $W = 3.08 \text{ kWh}/(\text{Nm}^3 \text{H}_2)$. The main advantage of the SOE is significantly lower specific electricity consumption as compared with that of low temperature electrolyzers. For example, $W = 4.2 \div 4.8 \text{ kWh}/(\text{Nm}^3 \text{H}_2)$ in alkaline electrolyzers [28] and $W = 4.5 \text{ kWh}/(\text{Nm}^3 \text{H}_2)$ in PEM electrolyzers [29].

When the SOE operates in the endothermic mode, the electrical efficiency of the SOE is greater than 100 %. There is no violation of the conservation law here: if we take into account the consumed thermal energy, the total efficiency will be less than 100 %.

A feature of the SOE is the possibility of electrochemical decomposition of carbon dioxide, which occurs according to the reaction



Simultaneous electrolysis of water vapor and carbon dioxide, called co-electrolysis, can be used to regenerate oxygen in life support systems for closed compartments. Another aim of co-electrolysis is production of synthesis gas (a mixture of H_2 and CO) from flue gases, followed by the production of artificial fuels using organic synthesis. The formula for calculating the EMF in this case is

$$E = X_H E_H + X_C E_C, \quad (10)$$

where X_H is a part of hydrogen-containing and X_C of carbon-containing components in the cathode gas mixture, E_C is EMF calculated by the formula

$$E_C = \left(\frac{RT}{2F} \right) \ln \left(\frac{K_2 p_{CO}}{p_{CO_2}} \right), \quad (11)$$

where K_2 is the equilibrium constant of CO oxidation reaction.

Long-term test of a SOE single cell for steam electrolysis was carried out for 23 thousand hours at 850 °C and current density of 0.9 A/cm² [30]: the voltage growth rate was 0.57 %/1000 h. In [31] the results of testing a single cell of the SOE for 34 thousand hours are given. The tests were carried out at a current density of 0.6 A/cm² at an initial temperature of 780 °C and a voltage close to thermoneutral one (1.29 V). Due to the degradation of the SOE components properties, the current density decreased with time. To maintain a constant current density of the cell, a stepwise increase in temperature was carried out. At the end of the tests the temperature was 805 °C, the rate of its change was 0.8–0.9 °C/1000 h. Such rates of temperature change make it possible to predict a resource of more than 80 thousand hours, if we assume that the SOE temperature should not exceed 850 °C.

3. Solid oxide fuel cells (SOFCs)

An SOFC transforms chemical energy of fuel to electrical energy and heat. Pure hydrogen or a mixture of hydrogen and carbon monoxide (CO) can be used as a fuel for the SOFC. Such a mixture can be produced by reforming or partial oxidation of hydrocarbons. The SOFC design is analogous to the design of SOE. However, the electrode processes in the SOFC are opposite to those in the SOE. Reactions inverse to (1) and (9) occur at the

SOFC fuel electrode (anode), and the reaction inverse to (2) occurs at the SOFC oxygen electrode (cathode). The current density in the cross-section of SOFC, x , is calculated by the formula

$$i(x) = \frac{(E(x)-U)}{\rho^*} \quad (12)$$

The electromotive force is calculated by the following formula:

$$E = X_H E_H + X_C E_C + E_{air}, \quad (13)$$

where $E_{air} = \left(\frac{RT}{4F}\right) \ln(p_{O_2})$ is additional term, taking into account that, as a rule, air is supplied to the SOFC cathode channel, p_{O_2} is the partial pressure of oxygen in the air. As the fuel moves in the anode channel, its concentration decreases, and the concentration of oxidized components (H_2O and CO_2) increases, which leads to a decrease in the EMF and current density. Complete oxidation of fuel in the SOFC is impossible, the degree of fuel utilization is characterized by the utilization factor η_f , that is equal to the ratio of the consumed charge, q , to the charge corresponding to the complete oxidation of one mole of fuel, zF . $z=2$ for H_2 and CO , and $z=8$ for CH_4 . Usually, $\eta_f \approx 0.9$. In practice, it is important to know the average value of the current density, that can be calculated from equation (12) using the average value of the EMF, which decreases from 953 mV at 750 °C to 909 mV at 900 °C if $\eta_f = 0.9$.

The SOFC efficiency is defined as the ratio of the generated electricity ($W=qU$) to the chemical energy of the consumed fuel:

$$\eta = \frac{qU}{-\Delta H_{298}} \quad (14)$$

By multiplying the numerator and denominator in (13) by $-\Delta H_{298}$ and using the formula (7), one can obtain a formula for calculating the SOFC efficiency

$$\eta = \eta_f \frac{U}{U_{th,298}} \quad (15)$$

Modern SOFCs operate at a cell voltage of 0.8 V, therefore, when hydrogen is used as a fuel, $\eta = 0.58$. When using methane as a primary fuel, $U_{th,298} = -\Delta H_{CH_4,298}/8F = 1.034$ V. At the same output voltage in this case $\eta = 0.7$.

Long-term tests of two-cell SOFC mini-stack were carried out in 2007–2019 for more than 100 thousand hours at a temperature of 700 °C [32]. First 40 thousand hours (the first stage), the voltage of the cells decreased from 0.8 to 0.45 V. The average rate of voltage degradation at a constant current density of 0.5 A/cm² was 0.5 %/1000 hours, and at the first stage it amounted to 1 %/1000 hours, then, at the final stage, the rate of voltage degradation was 0.2 %/1000 hours. The authors attribute the high degradation rates at the first stage to the

poor choice of the protective layer composition (MnO_x , as indicated in the article) on the interconnector used in this test. Tests of a four-cell stack, in which a manganese-cobalt-ferrite spinel was used to protect the interconnector, conducted later for 34 thousand hours at 700 °C and a current density of 0.5 A/cm² showed a voltage degradation of 0.3 %/1000 hours [33]. It should be noted that hydrogen with a moisture content of 12–20 % was used as fuel in these tests and the degree of its utilization was low (40 %), which is far from parameters acceptable for practical use. However, this does not detract from the importance of the obtained results of long-term tests, which make it possible to predict the possibility of creating an SOFC with a service life of up to 100 thousand hours.

4. Cells based on protonic ceramic electrolytes

Reducing the operating temperature of electrochemical cells based on solid oxide electrolytes down to 400–700 °C makes possible to create so-called “intermediate-temperature” electrochemical energy conversion devices where a wider range of cheaper materials for interconnects, sealing, gas-service pipes, etc, can be used.

In recent decades, protonic ceramic electrolytes have been considered as promising means for such devices, since they have a higher electrical conductivity in this temperature range compared to solid oxide electrolytes with oxygen-ion conductivity. The examples of the protonic ceramic electrolytes are doped cerates and zirconates of the perovskite structure [34]. The main disadvantage of such electrolytes is partial non-ionic conductivity, namely, hole conductivity in an oxidizing environment.

4.1. Protonic ceramic electrolysis cells (PCECs)

In the case of PCEC, the theoretical EMF is calculated by the equation

$$\eta E_H = \frac{RT}{2F} \ln \frac{p_{H_2}^{cat}}{p_{H_2}^{an}} \quad (16)$$

where $p_{H_2}^{cat}$ and $p_{H_2}^{an}$ – partial pressures of hydrogen at the cathode and anode, respectively. The partial pressure of hydrogen at the cathode is equal to its mole fraction, the same parameter at the anode is calculated by the formula:

$$p_{H_2}^{an} = \frac{p_{H_2O}}{p_{O_2}^{1/2} K_1} \quad (17)$$

where K_1 is the equilibrium constant of the hydrogen oxidation reaction.

When the voltage U is applied to a protonic ceramic cell, a proton current density in the cross-section x of the cell is determined by the equation

$$i_H(x) = (U - E_H(x)) \cdot \sigma_H^*(x), \quad (18)$$

where $\sigma_H^*(x)$ is a proton conductivity of 1 cm² of the cell, $\sigma_H = \sigma \cdot t_H$ is a proton conductivity of the electrolyte, σ is a total conductivity of the electrolyte and t_H is the proton transfer number. The last value is often defined as the ratio of the measured EMF to the theoretical one.

Here we accept that the polarization of electrodes is negligible. Proton conductivity in the protonic ceramic electrolyte depends on steam partial pressure according to the proportion

$$\sigma_H \sim p_{H_2O}^{1/2}. \quad (19)$$

Consequently, from the cathode side, the proton conductivity decreases along the steam flow. In order to keep proton conductivity at an appropriate level it is necessary to add some steam into the anode space. In general, the calculation of the proton current density distribution along the cell is a difficult task.

The partial non-ionic conductivity in protonic ceramic cells affects its electrical efficiency. The latter can be calculated using the formula

$$\eta_{el} = \eta_F \frac{U_{th}}{U}, \quad (20)$$

where η_F is a part of electrical energy spent on the electrochemical transformation called the Faradaic efficiency. In the case of a protonic ceramic electrolytic cell, the Faradaic efficiency is equal to a ratio of the proton current to the total current:

$$\eta_F = \frac{(U - E_H^*) \cdot \sigma_H^*}{(U - E_H^*) \cdot \sigma_H^* + U \cdot \sigma_h^*}. \quad (21)$$

The numerator is the average proton current density obtained by modifying Eq. (18), and the denominator is the average total current density. The Faradaic efficiency, and hence the electrical efficiency, is highly dependent on the proton transfer number. For example, if $t_H = 0.98$ then $\eta_F = 0.94$, and if $t_H = 0.95$ then $\eta_F = 0.84$. When an ion transfer number is equal to unit and the cell operates under the thermoneutral regime, the specific electrical energy demand is 3.08 kWh/Nm³H₂. At $t_H = 0.98$ this value increases up to 3.3 and at $t_H = 0.95$ up to 3.7 kWh/Nm³H₂, which corresponds to the $\eta_F = 0.83$. Correspondingly, the consumption of electricity increases. In fact, well-known protonic ceramic electrolytes have the proton transfer number lower 0.95 when operate under electrolysis mode [35]. For example, experiments with PCEC showed that the Faradaic efficiency was 0.76 [36].

4.2. Protonic ceramic fuel cells (PCFCs)

PCFCs demonstrate high performance at low temperatures. In [37], it was reported that the cell based on stoichiometric BaZr_{0.4}Ce_{0.4}Y_{0.1}Yb_{0.1}O_{3-δ} exhibited 1.90 Wcm⁻² at 650 °C and 1.01 Wcm⁻² at 550 °C with humidified H₂ at the anode and air at the cathode. This is

very impressive characteristics, however, due to the partial hole conduction, the efficiency of the PCFCs will be lower than that of the SOFCs. The open circuit voltage (OCV) of the PCFCs is lower than the theoretical one and some part of the fuel is wasted on generating a useless hole current. As a first approximation, the PCFC efficiency can be calculated using the following formula:

$$\eta = \frac{t_H \eta_f U}{U_{tn,298}}. \quad (22)$$

It was theoretically shown that methane can be used as a primary fuel in a fuel cell based on a solid oxide protonic electrolyte [38]. However, as the fuel processor temperature has to be higher than 700 °C for effective methane reforming, it cannot receive heat from the PCFC at lower temperatures, additional heat is required and additional fuel has to be used, reducing the fuel cell efficiency. Therefore, the only suitable fuel for PCFCs at temperatures below 700 °C is hydrogen.

5. Conclusions

The features of the operation of solid oxide electrolytic devices of high productivity and the issues of their economic performance today require intensive study. For the practical implementation of electrolyzers and fuel cells in the industrial power industry, work will be required to create models of various levels that require knowledge of the main parameters of these devices considered in this paper.

Supplementary materials

No supplementary materials are available.

Funding

This research had no external funding.

Acknowledgments

None.

Author contributions

Anatoly Demin: Conceptualization; Writing – original draft & Editing. Dmitry Bronin: Review & Editing.

Conflict of interest

The authors declare no conflict of interest.

Additional information

Anatoly Demin, Scopus ID: 13805326000; Web of Science ResearcherID: F-3468-2017.

Dmitry Bronin, Scopus ID: 6701491633; Web of Science ResearcherID: K-5581-2018.

References

1. Legasov VA, Ponomarev-Stepnoy NN, Protsenko AN, Chernilin YuF et al., Atomno-vodorodnaya energetika (prognоз развития) [Nuclear-hydrogen energy (development forecast)], Questions of Nuclear Science and Technology (Nuclear-Hydrogen Energy) 1 (1976) 5–34 (in Russian).
2. Ponomarev-Stepnoy NN, Stolyarevskii AYa, Pakhomov VP, Atomno-vodorodnaya energetika [Nuclear-Hydrogen Energy], Nuclear Energy 96 (6) (2004) 411–425 (in Russian). Available from: http://elib.biblioatom.ru/text/atomnaya-energiya_t96-6_2004/go_3/, Accessed on 14 June 2023.
3. Graves C, Ebbesen SD, Mogensen M, Lackner KS, Sustainable hydrocarbon fuels by recycling CO₂ and H₂O with renewable or nuclear energy, Renewable Sustain. Energy Rev. 15 (1) (2011) 1–23. <https://doi.org/10.1016/j.rser.2010.07.014>
4. Perfiliev MV, Demin AK, Kuzin BL, Lipilin AS, Vysokotemperaturnii electroliz gazov [High-Temperature Gas Electrolysis]. Nauka: Moscow; 1988. 232 p. (in Russian).
5. Laguna-Bercero MA, Recent advances in high temperature electrolysis using solid oxide fuel cells: A review, J. Power Sources 203 (2012) 4–16. <https://doi.org/10.1016/j.jpowsour.2011.12.019>
6. Hino R, Haga K, Aita H, Sekita K, R&D on hydrogen production by high-temperature electrolysis of steam, Nuclear Eng. Design 233 (1–3) (2004) 363–375. <https://doi.org/10.1016/j.nucengdes.2004.08.029>
7. Forsberg C, Futures for hydrogen produced using nuclear energy, Progress in Nuclear Energy 47 (1–4) (2005) 484–495. <https://doi.org/10.1016/j.pnucene.2005.05.049>
8. Utgikar V, Thiesen T, Life cycle assessment of high temperature electrolysis for hydrogen production via nuclear energy, Int. J. Hydrogen Energy 31 (7) (2006) 939–944. <https://doi.org/10.1016/j.ijhydene.2005.07.001>
9. Harvego EA, McKellar MG, O'Brien JE, Herring JS, Parametric evaluation of large-scale high-temperature electrolysis hydrogen production using different advanced nuclear reactor heat sources, Nucl. Eng. Design 239 (9) (2009) 1571–1580. <https://doi.org/10.1016/j.nucengdes.2009.03.003>
10. Stoots CM, O'Brien JE, Condie KG, Hartvigsen JJ, High-temperature electrolysis for large-scale hydrogen production from nuclear energy - experimental investigations, Int. J. Hydrogen Energy 35 (10) (2010) 4861–4870. <https://doi.org/10.1016/j.ijhydene.2009.10.045>
11. O'Brien JE, Large scale hydrogen production from nuclear energy using high temperature electrolysis. In: Proc. 14th International Heat Transfer Conference; 2010 August 3–18; Washington D.C., USA. 23341.
12. Zhang W, Yu B, Xu J, Efficiency evaluation of high-temperature steam electrolytic systems coupled with different nuclear reactors, Intern. J. Hydrogen Energy 37 (17) (2012) 12060–12068. <https://doi.org/10.1016/j.ijhydene.2012.04.024>
13. Giraldi MR, Francois J-L, Martin-del-Campo C, Life cycle assessment of hydrogen production from a high temperature electrolysis process coupled to a high temperature gas nuclear reactor, Intern. J. Hydrogen Energy 40 (10) (2015) 4019–4033. <https://doi.org/10.1016/j.ijhydene.2015.01.093>
14. El-Emam RS, Khamis I, International collaboration in the IAEA nuclear hydrogen production program for benchmarking of HEEP, Intern. J. Hydrogen Energy 42 (6) (2017) 3566–3571. <https://doi.org/10.1016/j.ijhydene.2016.07.256>
15. Milewski J, Kupecki J, Szczęśniak A, Uzunow N, Hydrogen production in solid oxide electrolyzers coupled with nuclear reactors, Intern. J. Hydrogen Energy 46 (72) (2021) 35765–35776. <https://doi.org/10.1016/j.ijhydene.2020.11.217>
16. Calipse F, Cappiello FL, Cimmino L, Vicidomini M, Dynamic simulation modeling of reversible solid oxide fuel cells for energy storage purpose, Energy 260 (2022) 124893. <https://doi.org/10.1016/j.energy.2022.124893>
17. Koh JH, Yoon DJ, Oh CH, Simple electrolyzer model development for high-temperature electrolysis system analysis using solid oxide electrolysis cell, J. Nucl. Sci. Techn. 47 (7) (2010) 599–607. Available from: <https://www.tandfonline.com/doi/abs/10.1080/18811248.2010.9720957>, Accessed on 14 June 2023.
18. Minh NQ, Mogensen MB, Reversible solid oxide fuel cell technology for green fuel and power production, Interface 22 (4) (2013) 55–62. <https://doi.org/10.1149/2.F05134if>
19. Di Giorgio P, Desideri U, Potential of reversible solid oxide cells as electricity storage system, Energies 9 (8) (2016) 662. <https://doi.org/10.3390/en9080662>
20. Osinkin DA, Bogdanovich NM, Beresnev SM, Pikalova EYu et al., Reversible solid oxide fuel cell for power accumulation and generation, Russian J. Electrochem. 54 (8) (2018) 644–649. <https://doi.org/10.1134/S1023193518080050>
21. Venkataraman V, Pérez-Fortes M, Wang L, Hajimolana YS et al., Reversible solid oxide systems for energy and chemical applications – Review & perspectives, J. Energy Storage 24 (2019) 100782. <https://doi.org/10.1016/j.est.2019.100782>
22. Zheng W, Zhang M, Li Y, Shao Z, Wang X, Optimal dispatch for reversible solid oxide cell-based hydrogen/electric vehicle aggregator via stimuli-responsive charging decision estimation, Intern. J. Hydrogen Energy 47 (13) (2022) 8502–8513. <https://doi.org/10.1016/j.ijhydene.2021.12.157>
23. Graves C, Ebbesen SD, Jensen SH, Simonsen SB, Mogensen MB, Reversible SOFC degradation eliminating degradation in solid oxide electrochemical cells by reversible operation, Nature Materials 14 (2) (2015) 239–244. <https://doi.org/10.1038/nmat4165>
24. Yu M, Tong X, Sudireddy BR, Chen M, Performance and durability of reversible solid oxide cells with nano-electrocatalysts infiltrated electrodes, JOM 74 (2022) 4495–4595. <https://doi.org/10.1007/s11837-022-05540-5>
25. Sampathkumar SN, Aubin Ph, Couturier K, Sun X, Sudireddy BR et al., Degradation study of a reversible solid oxide cell (rSOC) short stack using distribution of relaxation times (DRT) analysis, Intern. J. Hydrogen Energy 47 (18) (2022) 10175–10193. <https://doi.org/10.1016/j.ijhydene.2022.01.104>
26. Yang C, Guo R, Jing X, Li P et al., Degradation mechanism and modeling study on reversible solid oxide cell in dual-mode – A review, J. Hydrogen Energy 47 (89) (2022) 37895–37928. <https://doi.org/10.1016/j.ijhydene.2022.08.240>
27. Buttler A, Spliethoff H, Current status of water electrolysis for energy storage, grid balancing and sector coupling via power-to-gas and power-to-liquids: A review, Renewable Sustain. Energy Rev. 82 (3) (2018) 2440–2454. <https://doi.org/10.1016/j.rser.2017.09.003>

28. David M, Ocampo-Martinez C, Sánchez-Peña R, Advances in alkaline water electrolyzers: A review, *J. Energy Storage* **23** (2019) 392–403. <https://doi.org/10.1016/j.est.2019.03.001>
29. Anghilante R, Colomar D, Brisse A, Marrony M, Bottom-up cost evaluation of SOEC systems in the range of 10–100 MW, *Intern J Hydrogen Energy* **43** (45) (2018) 20309–20322. <https://doi.org/10.1016/j.ijhydene.2018.08.161>
30. Schefold J, Brisse A, Poepke H, 23,000 h steam electrolysis with an electrolyte supported solid oxide cell, *Intern. J. Hydrogen Energy* **42** (19) (2017) 13415–13426. <https://doi.org/10.1016/j.ijhydene.2017.01.072>
31. Schefold J, Poepke H, Brisse A, Solid oxide electrolyser cell testing up to the above 30,000 h time range, *ECS Trans.* **97** (7) (2020) 553–563. <https://doi.org/10.1149/MA2020-0136l45lmtgabs>
32. Fang Q, Blum L, Stolten D, Electrochemical performance and degradation analysis of an SOFC short stack following operation of more than 100,000 hours, *ECS Transactions* **91** (1) (2019) 687–696. <https://doi.org/10.1149/09101.0687ecst>
33. GroB-Barsnick SM, Fang Q, Batfalsky P, Niewolak L, Blum L, Quadakkers WJ, Post-test characterization of metallic materials and adjacent components in an SOFC stack after 34,000 h operation at 700 °C, *Fuel Cells* **19** (1) (2019) 84–95. <https://doi.org/10.1002/fuce.201800050>
34. Kasyanova AV, Zvonareva IA, Tarasova NA, Bi L, et al., Electrolyte materials for protonic ceramic electrochemical cells: Main limitations and potential solutions, *Materials Reports: Energy* **2** (4) (2022) 100158. <https://doi.org/10.1016/j.matre.2022.100158>
35. Heras-Juaristi G, Perez-Coll D, Mather GC, Temperature dependence of partial conductivities of the BaZr_{0.7}Ce_{0.2}Y_{0.1}O_{3-δ} proton conductor, *J. Power Sources* **364** (2017) 52–60. <https://doi.org/10.1016/j.jpowsour.2017.08.011>
36. Choi S, Davenport TC, Haile SM, Protonic ceramic electrochemical cells for hydrogen production and electricity generation: Exceptional reversibility, stability, and demonstrated faradaic efficiency, *Energy Environ. Sci.* **12** (2019) 206–215. <https://doi.org/10.1039/C8EE02865F>
37. Choi M, Paik J, Kim D, Woo D, et al., Exceptionally high performance of protonic ceramic fuel cells with stoichiometric electrolytes, *Energy Environ. Sci.* **14** (2021) 6476–6483. <https://doi.org/10.1039/DIEE01497H>
38. Demin AK, Tsiaikaras PE, Sobyanin VA, Hramova SY, Thermodynamic analysis of a methane fed SOFC system based on a protonic conductor, *Solid State Ionics*, **152–153** (2002) 555–560. [https://doi.org/10.1016/S0167-2738\(02\)00363-6](https://doi.org/10.1016/S0167-2738(02)00363-6)